

## Article

# Cation–Anionic Interactions of Dyes in Aqueous Solutions: Bromocresol Purple in the Processes of Dissimilar Association

Serghey A. Shapovalov 

Research Institute of Chemistry, V. N. Karazin Kharkiv National University, Svobody sq. 4, 61022 Kharkiv, Ukraine; serghey.a.shapovalov@karazin.ua

**Abstract:** The interaction between single- or double-charged anions of bromocresol purple (BP) and cyanine cations (quinaldine blue, QB, or quinaldine red, QR) at concentrations of dyes  $5.0 \cdot 10^{-7}$ – $4.0 \cdot 10^{-5}$  mol/L has been investigated by vis-spectroscopy. The thermodynamic constants of dissimilar associations ( $K_{as}$ ) have been studied. Comparison of the values of  $\lg K_{as}$  shows that  $QB^-$  associates of  $BP^-$  are more stable ( $6.61 \pm 0.07$ ) than QR associates ( $4.84 \pm 0.06$ ); a similar phenomenon is observed for associates of the  $BP^{2-}$  anion. Semi-empirical calculations (PM3 method) are in agreement with the vis-spectroscopy data and indicate that the association of dye into an associate is possible. The standard enthalpies of formation of associates ( $\Delta_f H^\circ$ ) and energy diagrams have been determined. The  $\Delta_f H^\circ$  data indicate that the formation of an associate between dye ions is an energetically favourable process. The gain in energy significantly exceeds the systematic error of semi-empirical calculations and increases from 157 kJ/mol (associate “ $BP^- + QB^-$ ”) to 729 kJ/mol (associate “ $BP^{2-} + QR^+$ ”). The most probable structures of dissimilar associates are presented. The study of the dissimilar association develops the concept of intermolecular interactions in solutions.

**Keywords:** bromocresol purple; dissimilar association; vis-spectroscopy; enthalpy of formation; semi-empirical method



**Citation:** Shapovalov, S.A.

Cation–Anionic Interactions of Dyes in Aqueous Solutions: Bromocresol Purple in the Processes of Dissimilar Association. *Colorants* **2022**, *1*, 5–19. <https://doi.org/10.3390/colorants1010003>

Academic Editor: Anthony Harriman

Received: 31 October 2021

Accepted: 14 December 2021

Published: 22 December 2021

**Publisher’s Note:** MDPI stays neutral with regard to jurisdictional claims in published maps and institutional affiliations.



**Copyright:** © 2021 by the author. Licensee MDPI, Basel, Switzerland. This article is an open access article distributed under the terms and conditions of the Creative Commons Attribution (CC BY) license (<https://creativecommons.org/licenses/by/4.0/>).

## 1. Introduction

Sulfonephthalein dyes have a wide range of applications, from acid–base or met-allochromic indicators to analytical reagents for spectral determination of a number of organic substances [1–3]. The bromine derivatives attract attention due to favorable specific features, such as the stability of protolytic forms, weak dimerization, good diversity of absorption bands of single- and double-charged anions, and high contrast of color reactions [3,4]. In particular, they are used in technologies for determining the acidity of pure and natural waters [5–7] and are also the basis of sensitive elements of optical pH sensors, fiber optic biosensors, and chips [8–11]. Quantitative determination of components in bio- and pharmaceuticals is one of the most promising areas of their application as analytical reagents: Antimicrobial, antihistamines, bactericidal, antidepressants, and others [12–26].

The effective use of 3,3′-dimethyl-5,5′-dibromophenolsulfonephthalein (BP) in technologies is expanding [27–49]. It includes sensitive gas sensors [27,28], electrochemical DNA biosensors to the antitumor drug [39], highly efficient extraction of heavy metals from industrial effluents by adsorption on a modified zeolite surface [40], lysine decarboxylase analysis [41], the adsorption of hydrophobic molecules on the membrane of erythroleukemia cells [42], and evaluation of the properties of serum albumin [38,43–48] and extracellular lactase [49]. It is noteworthy that many applications are based on the formation of dissimilar associates between the anionic form of sulfonephthalein and the an-alyte. In some cases, associates are able to be extracted into the organic phase (chloroform, dichloromethane [12,13,15–19,21,24,26]).

Studies of the dissimilar association of sulfonephthaleines and other dyes are becoming practical. They provide information on the nature of physicochemical interactions and

the role of both chromophore fragments and functional groups. For example, it was found that the “dye + counterion” associates and the binding of each of them with biochemical receptors (with DNA [50,51] or proteins [52–54]) affect the action of medicinal agents; this problem has also been studied in the interaction of antibiotics with aromatic molecules (polyphenols, methylxanthines such as caffeine, etc.) [55]. Therefore, the dissimilar association is directly related to improving the effectiveness of pharmaceuticals. The analysis of publications indicates the need for in-depth study of cation–anionic interactions that cause the formation of associates, which include anions ( $\text{HAn}^-$ ,  $\text{An}^{2-}$ ) of BP or other sulfonephthalein dyes.

Various instrumental methods are used to study the association. At concentrations of interacting particles of  $1 \cdot 10^{-5}$  mol/L or more, it is known to use conductometry; however, this method is suitable for media with low dielectric constants. The most “sensitive” method is vis-spectroscopy (fluorimetry), which makes it possible to study the interactions of colored particles at concentrations  $1 \cdot 10^{-7}$ – $1 \cdot 10^{-4}$  mol/L.

The facts of the interaction of sulfonephthalein anions with cations ( $\text{Ct}^+$ ) of some dyes (rhodamines, cyanines) have been discussed previously [56–58]. However, the most probable structure of BP associates and their energy characteristics, in particular, the standard enthalpy of formation ( $\Delta_f H^\circ$ ), have not been studied. In this report, using the results of spectrophotometric measurements and quantum chemical calculations, we analyzed the cation–anion interactions that lead to the formation of stoichiometric associations between single or double-charged anions of BP and single-charged cations of polymethine dyes.

A systematic study of association in aqueous solution implies the use of such dyes that have satisfactory solubility and the ability to change light absorption upon association. Among the “standard” dyes that meet these requirements, attention is drawn to quinadine blue (QB) and quinadine red (QR). QB has a developed vibrational structure and a three-band absorption spectrum in water or organic solvents. Even a slight effect on the chromophore system, which has a counterion, changes its spectrum. A redistribution of the intensities of the absorption bands occurs, and frequency shifts appear. Such unique spectral properties have found application in methods for the qualitative and quantitative determination of a number of metals, in the study of the properties of polyelectrolytes, DNA, surfactants, and metal complex systems [3]. The observed spectral changes can also be linked to a certain type of formed particles in the process of heterogeneous association. However, the disadvantage of QB is the instability of its aqueous solutions. On the contrary, QR is more stable, although it does not have a developed vibrational structure. The advantage of QR is also the possibility to study the association in a wide range of concentrations since it is not as prone to self-association as QB.

Note that these cations have been used previously under the study of the processes of anionic dye association [57–59].

## 2. Materials and Methods

Disodium salts of sulfonephthaleins were used: QB was in the form of chloride salt, and QR was in the form of iodide salt (trademark “Merck KGaA”, Darmstadt, Germany; the content of the basic component was not less than 95%). The proper qualification of the chemical purity of the preparations of each of the dyes was verified spectrophotometrically, taking into account the known values of the molar absorption coefficient ( $\epsilon_{\text{max}}$ , L/(mol·cm)) and the maximum absorption band ( $\lambda_{\text{max}}$ ) for the most intensely colored of protolytic form. The acidity of the medium was created with phosphate, borate, acetate buffer solutions, and in some cases, hydrochloric acid or sodium hydroxide. Additional observations have shown that the addition of buffer solutions does not significantly affect the light absorption of dyes and association processes. The pH was monitored with a glass electrode. The ionic strength ( $I$ ) of the solutions did not exceed 0.004 mol/L. Distilled water was used to prepare the solutions with an electrical conductivity of no more  $4 \cdot 10^{-6}$  S. The values of the optical density, which are the basis for the calculations of the equilibrium constants of the association ( $K_{\text{as}}$ ), were checked for compliance with the basic law of light absorption. The

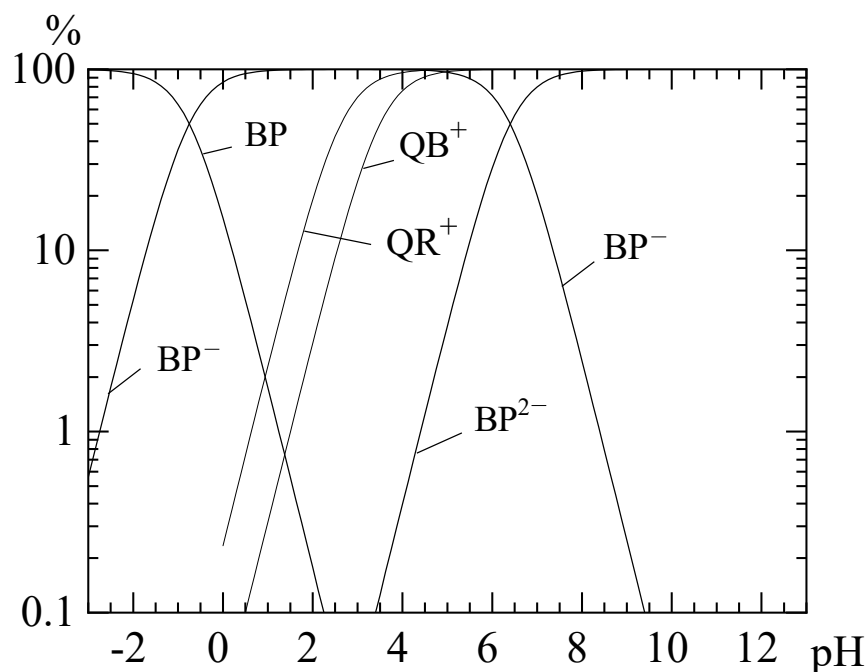
absorption spectra were measured on the upgraded spectrophotometer “Hitachi U3210”, Hitachi, Inc., Tokio, Japan (at room temperature) with an error value in determining the absorption wavelength of no more than  $\pm 0.5$  nm. It is experimentally verified that temperature fluctuations within 2–3 degrees practically do not affect the spectral properties of the studied dyes.

The methods of preparation of mixtures of dyes and the calculation of spectral and equilibrium characteristics of associates are covered in [56–58]. To calculate the standard enthalpies of the formation of dye ions and their associates, as well as to establish their structure, the semi-empirical quantum chemical method PM3 was used. The method is integrated into the software packages “HyperChem 8.0”, Hupercube, Inc., New York, NY, USA (*evaluation version*) and “MOPAC 2009”, Stewart Computational Chemistry, Colorado Springs, CO, USA. The principles of calculations for the structures of dyes and their ionic associates have been described in more detail previously [3,56,59,60].

### 3. Results

#### 3.1. Dyes in the Aqueous Solution

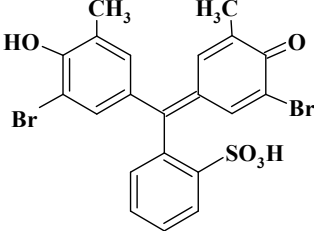
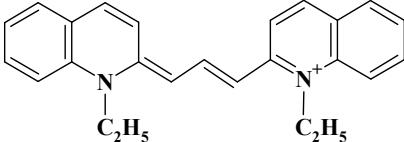
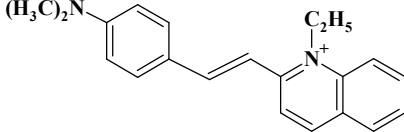
Under the study of the interaction of  $\text{HAn}^-$  (or  $\text{An}^{2-}$ ) with  $\text{Ct}^+$ , we adhered to the acidity of the solution, which would ensure the coexistence of the corresponding ionic forms (Figure 1). Otherwise, the interpretation of spectral changes is difficult due to possible interactions involving mixtures of proprietary dye forms.



**Figure 1.** The relative content of protolytic forms of dyes depending on the pH of the aqueous solution.

Upon creating the optimal acidity of the solution, the values of  $\text{p}K_{a1}$  and  $\text{p}K_{a2}$  were taken into account (see Table 1; the characteristics of BP and cyanine dyes are given for  $I \rightarrow 0$  according to [61,62]; the error of  $\text{p}K_a$  values is  $\pm(0.03\text{--}0.08)$ ); the values of  $\text{p}K_{a1}$  for QB and QR refer to the process of dissociation of the  $\text{HCt}^{2+}$  cation).

**Table 1.** Spectral and protolytic characteristics of dyes.

Dye	pK <sub>a1</sub> (λ <sub>max</sub> , nm HAn <sup>-</sup> or Ct <sup>+</sup> )	pK <sub>a2</sub> (λ <sub>max</sub> , nm An <sup>2-</sup> )
3,3-bis(3-bromo-4-hydroxy-5-methylphenyl)- 3H-2,1λ <sup>6</sup> -benzoxathiole-1,1-dione (BP) CAS 115-40-2 	-0.75	6.40
1-ethyl-2-[3-(1-ethyl-1,2-dihydroquinolin-2-ylidene) prop-1-en-1-yl]quinolin-1-ium chloride (QB <sup>+</sup> ) CAS 2768-90-3 	3.5 (600, α-band; 550, β-band)	-
2-(4-dimethylamino)styryl)-1-ethylquinolinium iodide (QR <sup>+</sup> ) CAS 117-92-0 	2.63 (528)	-

### 3.2. Spectral Properties of the Dyes

Features of BP and the cyanines are the following: (1) Dyes form stable protolytic forms in aqueous solutions; (2) dyes are able to associate at concentrations not exceeding their solubility in water; (3) ionic forms have a sufficient color intensity and the ability to significantly change the light absorption during association, which allows the study of quite small concentrations of interacting particles.

Interpretation of spectral changes from the standpoint of the equilibrium approach (using the law of active masses) implies compliance with the basic law of light absorption by protolytic forms of interacting dyes. The absorption spectra of aqueous BP solutions were investigated in the concentration range of  $4.96 \cdot 10^{-6}$  to  $4.96 \cdot 10^{-5}$  mol/L using a buffer solution and without the addition of salt additives or an organic solvent. The Savitsky–Goley procedure was used to smooth the electronic spectra [63,64]. The dependence of  $A_\lambda$  on the BP concentration for  $\lambda_{\max} = 431$  nm is a line passing through the origin. The linear regression equation has the form:

$$A_{431} = 0.00047_{(0.0043)} + 24798.1_{(139.8)} \times C_{BP}$$

The correlation coefficient is equal to 0.99, and its standard deviation is 0.0038. The free term of the regression equation (in parentheses) is statistical zero. This nature of the dependence obeys the basic law of light absorption and gives one reason to believe that in the studied range of concentrations, the single-charge BP anion is not prone to dimerization. It is experimentally set that this also applies to the double-charged ion BP.

Sulfonephthalein dyes are characterized by a number of protolytic transformations:  $H_3An^+ \rightleftharpoons H_2An^0 \rightleftharpoons HAn^- \rightleftharpoons An^{2-}$ . Cationic and neutral protolytic forms exist only in a strongly acidic environment. Anions, especially  $An^{2-}$ , have the most intense color; the light

absorption bands of  $\text{HAn}^-$  and  $\text{An}^{2-}$  forms are well spectrally spaced ( $\lambda_{\max}(\text{HAn}^-) = 430 \text{ nm}$ ,  $\lambda_{\max}(\text{An}^{2-}) = 588 \text{ nm}$  with molar absorption coefficients  $\epsilon_{\max}(\text{HAn}^-) = 24,900 \text{ L}/(\text{mol}\cdot\text{cm})$ ,  $\epsilon_{\max}(\text{An}^{2-}) = 67,200 \text{ L}/(\text{mol}\cdot\text{cm})$ ). This contributes to the experimental study of the ionic association of dyes at particle concentrations at the level of  $5 \cdot 10^{-6} \text{ mol/L}$ . It is noteworthy that the coefficient of the linear regression equation practically coincides in value with the given  $\epsilon_{\max}(\text{HAn}^-)$ . This indicates that only one protolytic form of BP exists at a certain acidity of the solution in the aqueous solution. In turn, significant differences in the values of  $\text{p}K_{\text{a}1}$  and  $\text{p}K_{\text{a}2}$  (see Table 1) allow for regulating the acidity of the solution to create conditions under which the existence of only a single- or double-charged anion is possible.

The linear regression equation has the form in the concentration range of  $1.0 \cdot 10^{-6}$ – $1.0 \cdot 10^{-4} \text{ mol/L}$  for QR [59]:

$$A_{528} = -0.0038_{(0.015)} + 3.37 \cdot 10^4_{(324)} \times C_{\text{QR}}.$$

The correlation coefficient is equal to  $0.99_{(0.03)}$ . The value of the free regression term is statistical zero as in the case of BP anions.

For QB, in contrast to other dyes, the basic law of light absorption is fulfilled only at relatively low (not more than  $3 \cdot 10^{-6} \text{ mol/L}$ ) concentrations because QB is very prone to self-association [65]. It is spectrally manifested by a weakening of the absorption of the  $\alpha$ -band and an increase in the intensity of the  $\beta$ -band (see Table 1).

Aqueous solutions of single-charged cyanines are markedly discolored due to the processes of protonation (the formation of  $\text{HCt}^{2+}$  particles in acidic conditions) and hydrolysis (the occurrence of  $\text{CtOH}$  and the appearance of turbidity in an alkaline solution).

## 4. Discussion

### 4.1. Spectral and Equilibrium Properties of Dissimilar Associates

A significant decrease in the intensity of the light absorption bands is a characteristic feature of the formation of cation–anionic associates. It is most clearly observed if increasing amounts of BP are added to the constant content of cyanine dye and the light absorption is measured against a solution containing the same concentration of BP as in the dye mixture. An analysis of changes in the electronic absorption spectra of mixtures of  $\text{Ct}^+$  with  $\text{HAn}^-$  and  $\text{Ct}^+$  with  $\text{An}^{2-}$  leads to the conclusion that the principle of additivity of light absorption is violated. The absorption intensity ( $A$ ) of the mixture of interacting counterions becomes less than the total light absorption of individual dye ions. This phenomenon occurs regardless of the initial concentrations of anions or cations (in the above ranges), as shown in Figures 2 and 3. The intensity of the  $\alpha$ -band is greater than the  $\beta$ -band for QB in Figure 2. However, the situation is the opposite (see Figure 3), where the concentration of QB is much more (“ $\text{Ct}^+ + \text{An}^{2-}$ ” system). Such spectral shifts of the absorption bands in the absence of new or the splitting of existing bands suggest a solvate-separated type of dissimilar associate structure (in accordance with the general features of spectral shifts for dye associate systems [3,66]).

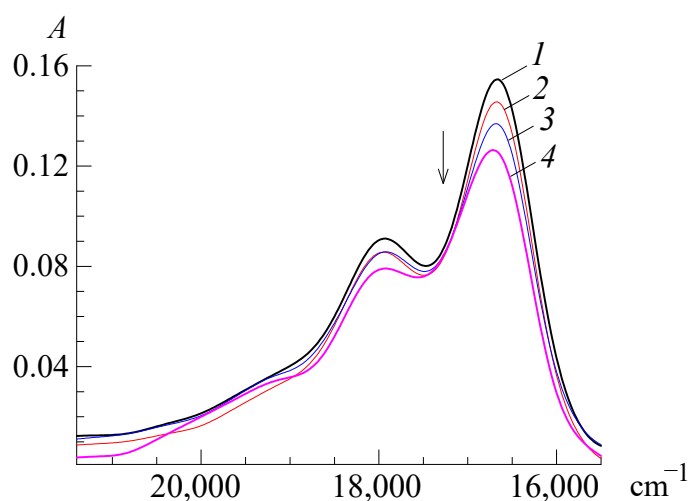


**Figure 2.** Absorption spectra in the system “BP + QB”. Concentrations, mol/L, QB:  $4.9 \cdot 10^{-7}$  (1–4); BP: 0 (1),  $2.30 \cdot 10^{-6}$  (2),  $8.30 \cdot 10^{-6}$  (3),  $4.51 \cdot 10^{-5}$  (4). The thickness of the absorbing layer ( $l$ ) is 5.00 cm, pH 9.2. Comparison solutions: Water (1), BP solution in the appropriate concentration (2–4).

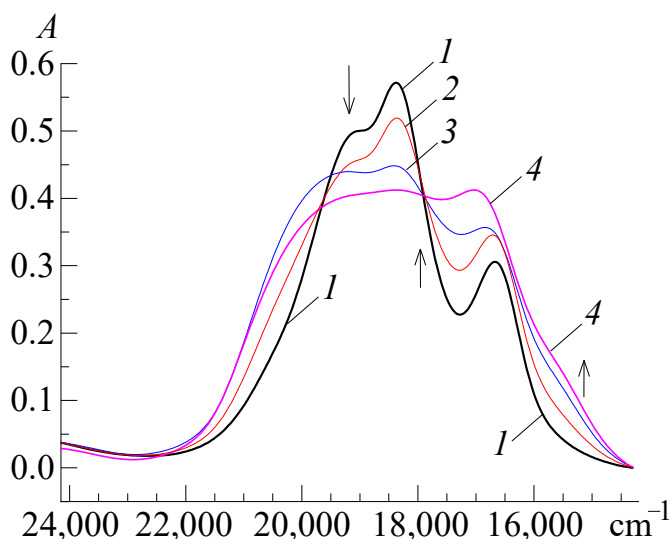


**Figure 3.** Absorption spectra in the system “BP + QB”. Concentrations, mol/L, QB:  $4.8 \cdot 10^{-5}$  (1–6); BP: 0 (1),  $1.1 \cdot 10^{-5}$  (2),  $2.2 \cdot 10^{-5}$  (3),  $3.03 \cdot 10^{-5}$  (4). The thickness of the absorbing layer ( $l$ ) is 0.20 cm, pH 9.2. Comparison solutions: Water (1), BP solution in the appropriate concentration (2–4).

Using methods for estimating the stoichiometric composition (similar to studies [12,13,56,60]), it was found that under certain conditions (such as initial concentrations of counterions and their molar ratios), anions of BP can form  $\text{Ct}^+$  associates of the composition  $\text{Ct}^+ \cdot \text{HAN}^-$  and  $(\text{Ct}^+)_2 \cdot \text{An}^{2-}$ . From the experimental data, it can be concluded that for dissimilar associates of BP, the stoichiometric ratio of QB: counterion is 1:1 for the case of the anion  $\text{HAN}^-$ , and it is 2:1 for the case of  $\text{An}^{2-}$ . For equilibria of type  $j\text{Ct}^+ + \text{An}^{j-} \rightleftharpoons (\text{Ct}^+)_j \cdot \text{An}^{j-}$ , the association constants ( $K_{\text{as}}$ ) were calculated taking into account the ratios of the stoichiometric coefficients. The concentration constant of the association  $K_{\text{as}}^{\text{conc.}}$  practically does not differ from the thermodynamic one  $K_{\text{as}}^{\text{thermod.}}$  because  $l \leq 0.004$  in all experiments:

$$K_{\text{as}}^{\text{thermod.}} = K_{\text{as}}^{\text{conc.}} = \frac{[(\text{Ct}^+)_j \cdot \text{An}^{j-}]}{(\text{C}_{\text{Ct}^+} - j \times [(\text{Ct}^+)_j \cdot \text{An}^{j-}])^j \times (\text{C}_{\text{An}^{j-}} - [(\text{Ct}^+)_j \cdot \text{An}^{j-}])}$$

where  $C_{Ct^+}$  is the initial molar concentration of the cationic dye (which does not change within the series);  $C_{An^{j-}}$  is the initial molar concentration of the anion;  $[(Ct^+)_j \cdot An^{j-}]$  is the equilibrium molar concentration of the associate (as):

$$[(Ct^+)_j \cdot An^{j-}] = \frac{C_{Ct} \times \varepsilon_{Ct} \times l + C_{An} \times \varepsilon_{An} \times l - A}{(j \times \varepsilon_{Ct} + \varepsilon_{An} - \varepsilon_{as}) \times l}$$

The last value was calculated on the principle of additivity of optical density  $A$  of a mixture of colored particles in the solution by the equation:

$$\begin{aligned} A &= A_{Ct} + A_{An} + A_{as} \text{ at a fixed wavelength } \lambda. \\ A_{Ct} &= [Ct] \times \varepsilon_{Ct} \times l = (C_{Ct} - j \times [(Ct^+)_j \cdot An^{j-}]) \times \varepsilon_{Ct} \times l, \\ A_{An} &= [An] \times \varepsilon_{An} \times l = (C_{An} - [(Ct^+)_j \cdot An^{j-}]) \times \varepsilon_{An} \times l, \\ A_{as} &= [(Ct^+)_j \cdot An^{j-}] \times \varepsilon_{as} \times l, \end{aligned}$$

where  $l$  is the thickness of the absorbing layer, cm.

For  $l = 1$  cm, it turns out:

$$[(Ct^+)_j \cdot An^{j-}] = \frac{C_{Ct} \times \varepsilon_{Ct} + C_{An} \times \varepsilon_{An} - A}{j \times \varepsilon_{Ct} + \varepsilon_{An} - \varepsilon_{as}}$$

In general, it is possible to use different ratios of cation and anion concentrations. However, when one of the dyes is susceptible to dimerization, then it is necessary to measure the optical density of the mixture at a constant concentration of this dye (for example, QB) and a varying concentration of the second dye (BP). In fact, the cationic dye is "titrated" by the anion, and then  $C_{Ct} \times \varepsilon_{Ct} \times l = \text{const}$ . If the absorption bands of the cation and the anion are well separated ( $\Delta\lambda_{\max} = |\lambda_{\max Ct} - \lambda_{\max An}| \geq 80 \dots 100$  nm), then the light absorption of the anion,  $A_{An}$ , at the selected wavelength  $\lambda_{\max Ct}$  barely differs from zero, since  $\varepsilon_{An} \sim 0$ . Then:

$$[(Ct^+)_j \cdot An^{j-}] = \frac{C_{Ct} \times \varepsilon_{Ct} - A}{j \times \varepsilon_{Ct} - \varepsilon_{as}}$$

where  $A$  is the measured value of the optical density of the dye mixture.

Data for  $K_{as}$  were obtained at  $C_{Ct^+} \approx 6 \cdot 10^{-7}$  mol/L for several  $C_{An^{j-}}$  values and at three wavelengths (see Table 2).

**Table 2.** The lg  $K_{as}$  values of BP associates.

Cation	lg $K_{as}$	
	$Ct^+ \cdot HAn^-$	$(Ct^+)_2 \cdot An^{2-}$
QB	$6.61 \pm 0.07$	$11.16 \pm 0.11$
QR	$4.84 \pm 0.06$	$8.29 \pm 0.05$

The obtained data on the logarithmic values of the association constant are in good agreement with the values of  $K_{as}$ , which were defined earlier by us [59] (QB:  $6.67 \pm 0.05$  ( $Ct^+ \cdot HAn^-$ ),  $11.07 \pm 0.10$  ( $(Ct^+)_2 \cdot An^{2-}$ ); QR:  $4.78 \pm 0.06$  and  $8.23 \pm 0.04$ , respectively) for slightly different concentration ranges of  $Ct^+$  and BP. This fact confirms the validity of considering the indicated stoichiometry of a dissimilar association from the position of an equilibrium model. However, it should be noted that turbidity may appear in more concentrated solutions of mixtures of dyes. This phenomenon indicates the formation of associates of more complex stoichiometry, which are sparingly soluble in water:  $(Ct^+)_j \cdot An^{j-} + kAn^{j-} (Ct^+)_j \cdot (An^{j-})_{k+1}$ . Thus, it is possible to form associates of complex composition by a cooperative mechanism, when the counterion interacts not only with the dye, but with the dissimilar associate. Similar facts were set earlier for tetraphenylborate

anion by spectrophotometrically [67] and for “daunomycin + ethidium bromide” [68] or “acridine orange + caffeine” [69] by  $^1\text{H}$  NMR spectroscopy.

Comparison of the values of  $\lg K_{\text{as}}$  (see Table 2) show that QB associates of BP are more stable than QR associates. This is probably due to the lower hydrophobicity of QR compared to QB. The octanol–water partition ratio is the most common way of expressing the hydrophobicity of a compound ( $P$ ), and it is defined as the ratio of the concentration of a solute in a water-saturated octanolic phase to its concentration in an octanol-saturated aqueous phase. The correlation between hydrophobicity and activity has provoked the extensive use of the octanol–water partition ratio, among others, as a descriptor in quantitative structure–activity/property relationships [70–73]. The higher the  $P$  parameter, the more hydrophobic the molecule is. Indices of hydrophobicity are  $\log P_{\text{QR}} = 5.15 \pm 0.12$  and  $\log P_{\text{QB}} = 5.69 \pm 0.12$  according to [74]. So, the manifestation of hydrophobic interactions in QR associates is reduced. In addition, the positive charge is localized mainly on the heteroatom of the nitrogen-containing heterocycle in QR, while the positive charge is delocalized in QB.

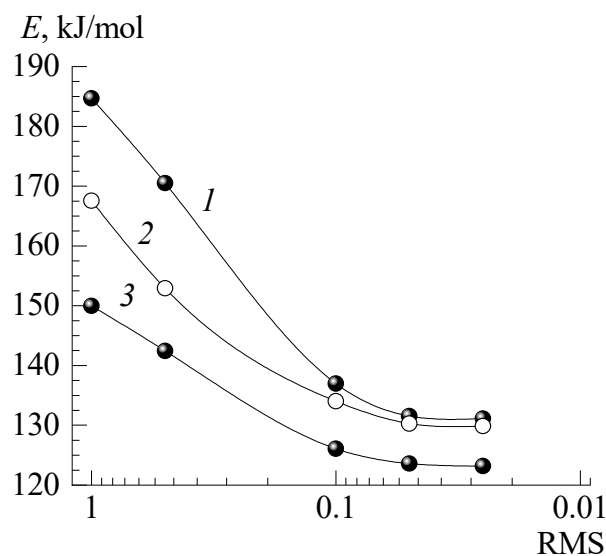
The formation of associates in solutions is more characteristic for dyes with a flat molecule shape and developed  $\pi$ -electronic fragments, which enhances the component of noncovalent interactions. Such properties have some thiocyanines, porphyrins, spiropyrans and squaraines [75–78]. However, sulfonephthaleins do not have a flat structure in contrast to these structures. However, the cation–anionic interactions for BP are significantly expressed as they follow from the determined values of  $K_{\text{as}}$ . Based on experimental data on stoichiometry, it can be assumed that the polymethine cation coordinates with the single-charge BP anion (or two cations coordinate with one double-charged BP anion). Using quantum chemical calculations, we considered the energy state (value of the standard enthalpy of formation,  $\Delta_f H^\circ$ ) of each of the counterions and associates in more detail, and also determined their most probable structure.

#### 4.2. Energy and Structural Properties of Dissimilar Associates

The semi-empirical PM3 method was used to estimate  $\Delta_f H^\circ$  values of ions and dissimilar associates. The parameters of this method most correctly reproduce the experimental values of  $\Delta_f H^\circ$  of organic compounds. It should be noted that  $\Delta_f H^\circ$  calculations for organic molecules by non-empirical methods lead to errors exceeding 100 kJ/mol even for small molecules, while the average error of the PM3 method in calculating  $\Delta_f H^\circ$  is only 25 kJ/mol [79,80]. In advance, the geometry of all structures was optimized by the method of molecular mechanics MM+ (by the minimum value of the total energy  $E$ ). This significantly simplified the further determination of  $\Delta_f H^\circ$  by the semi-empirical method.

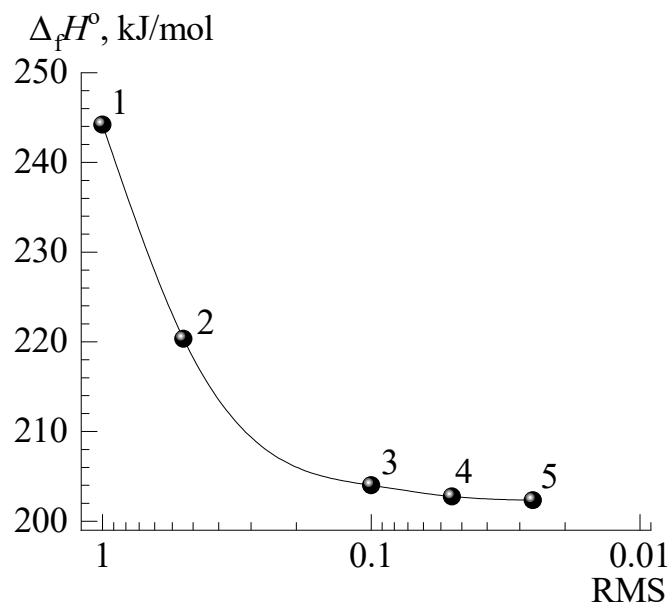
It is important to find the global energy minimum from a set of local minima to obtain the correct values of  $\Delta_f H^\circ$ . To do this, we tested several different starting locations (more often 5–6) of counterions in the associate. From the received calculated set of energy minima, the smallest was chosen; the energy of this structure corresponded to the global energy minimum. For example, Figure 4 shows three variants of the initial location of the two-charged ion in the association of  $\text{An}^{2-}$  with two cations of QR.

Different (1 and 2) starting positions of ions in an associate can lead to practically identical optimized values of  $E$ . However, in comparison with curve 3, this indicates that only a local energy minimum has been achieved, since in case 3 the energy results in being even lower. Thus, curve 3 corresponds to the variant with the energy of the global minimum  $E = 123$  kJ/mol.



**Figure 4.** Energy dependences on the RMS value for three variants (1–3) of different locations of ions in the  $(\text{Ct}^+)_2 \cdot \text{An}^{2-}$  associate.

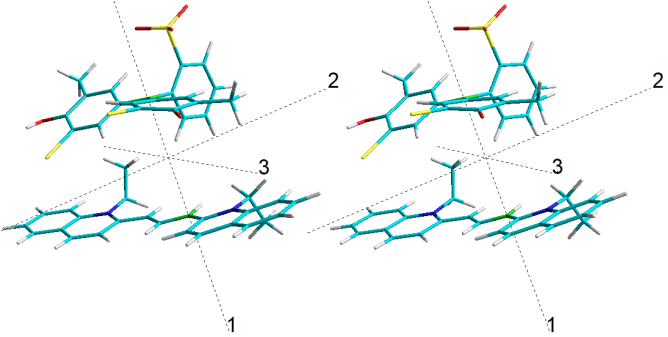
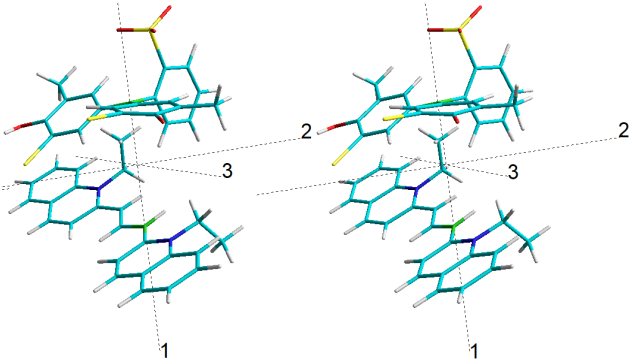
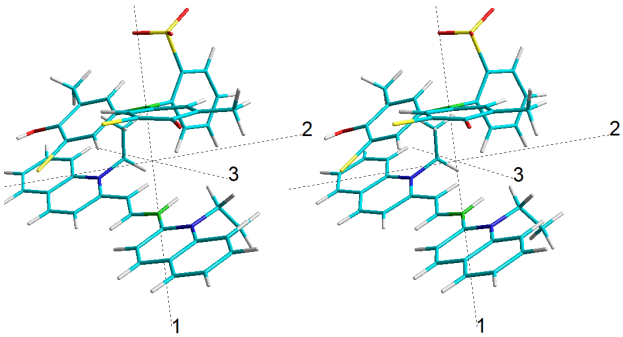
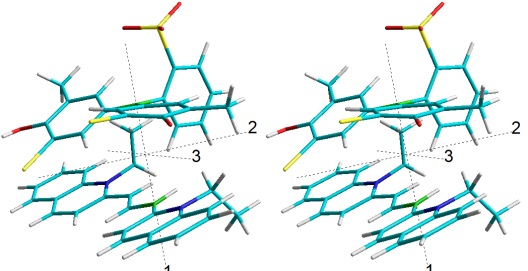
Note that the total energy gradient is calculated as a root mean square (RMS,  $\text{kJ}/(\text{mol} \cdot \text{Å})$ ) value. The gradient is the rate of change (first derivative) of total energy ( $E$ ) with respect to the displacement of each atom in the  $x$ ,  $y$ , and  $z$  directions; the local minimum of the potential energy of the structure is considered reached when  $\text{RMS} = 0$ . The process of finding the optimized variant of the associate structure was considered complete when the  $E$  or standard enthalpy of formation  $\Delta_f H^\circ$  ceased to depend on the RMS values. This is indicated by the flatness of the area of the corresponding graphical dependence (Figure 5).



**Figure 5.** Changes in  $\Delta_f H^\circ$  from RMS values for  $\text{Ct}^+ \cdot \text{HAN}^-$  associate of BP with QB, PM3 method.

Table 3 shows the dependence of  $\Delta_f H^\circ$  on RMS values, as well as changes in the location of ions during the optimization process (the numbers on the curve, Figure 5, correspond to the location of dyes from initial 1 to final 5 state; stereo images are presented, and 1, 2, 3 are the directions of the coordinate axes; the position of BP (BP is over) is conditionally fixed for clarity).

**Table 3.** Dependence of  $\Delta_f H^0$  on RMS values and change of mutual arrangement of BP and QR dyes in  $\text{Ct}^+ \cdot \text{HAN}^-$  associate.

State	Arrangement of BP and QB Ions
1	
2	
3	
4-5	

The optimization process is accompanied by a decrease in the distance between the dyes (the distance between the ions along the axis 1 is from 6.8 Å (initial state 1) to 4.2 Å (final state 5), a certain deformation  $\pi$ -electronic dye system, and is almost finalized with  $\Delta_f H^0 = 202$  kJ/mol at  $\text{RMS}_{\min} = 0.025$ .

The obtained data make it possible to build energy diagrams. The properties of the associate of the  $\text{HAN}^-$  anion with the QB cation are considered in Figure 6 as an example (numbers near the arrows indicate the range of variation of the values of  $\Delta_f H^0$ , kJ/mol).

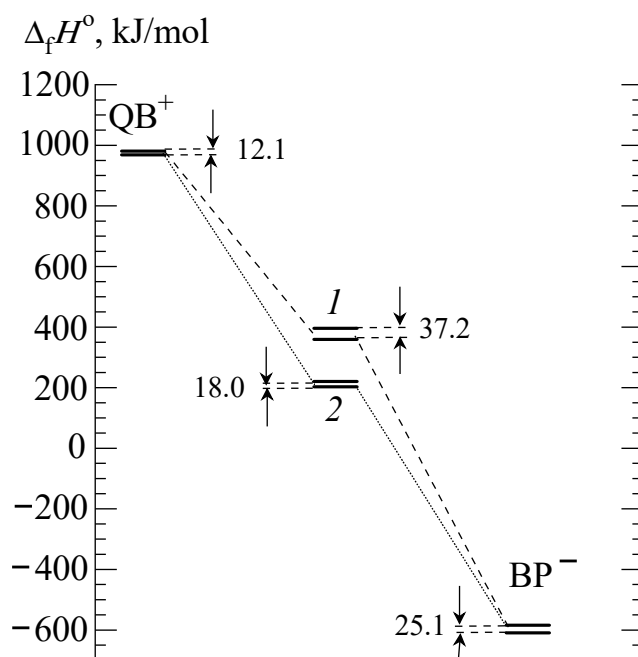


**Figure 6.** The value of  $\Delta_f H^\circ$  for ions ( $QB^+$ ,  $BP^-$ ) and the  $Ct^+ \cdot HAn^-$  associate.

The values of  $\Delta_f H^\circ$  980.8 ... 968.7 kJ/mol and  $-584.5 \dots -609.6$  kJ/mol correspond to  $Ct^+$  and  $HAn^-$  ions. Their algebraic sum ( $\Sigma$ ) can take values from  $980.8 - 584.5 = 396.3$  kJ/mol to  $968.7 - 609.6 = 359.1$  kJ/mol, that is it varies within  $396.3 - 359.1 = 37.2$  kJ/mol (level 1). The values of  $\Delta_f H^\circ$  for the  $Ct^+ \cdot HAn^-$  associate (level 2) are 220.4 ... 202.4 kJ/mol, that is these values differ by 18.0 kJ/mol (level 2). The differences between levels 1 and 2 are from  $359.1 - 220.4 = 138.7$  kJ/mol to  $396.3 - 202.4 = 193.9$  kJ/mol, which significantly exceeds the above systematic error of semi-empirical calculations. In this case, the relative error ( $\delta$ ) of the  $\Delta_f H^\circ$  estimate is no more than  $(193.9 - 138.7) \cdot 100\% / 193.9 \approx 28\%$ . These data indicate that the formation of an associate between dye ions is an energetically favorable process.

The  $\Delta_f H^\circ$  and  $\delta$  values are given for all dissimilar associates in Table 4 (rounded values).

**Table 4.** Values of  $\Delta_f H^\circ$ ,  $\Sigma - \Delta_f H^\circ$  and  $\delta$  for BP dissimilar associates.

An Associate	$\Sigma$ , kJ/mol	$\Delta_f H^\circ$ , kJ/mol	$\Sigma - \Delta_f H^\circ$ , kJ/mol/ $\delta$ , %
$QB^+ \cdot BP^-$	359	202	157/28
$QR^+ \cdot BP^-$	303	107	194/14
$(QB^+)_2 \cdot BP^{2-}$	1367	703	664/6
$(QR^+)_2 \cdot BP^{2-}$	1254	525	729/7

The analysis of the results leads to an important conclusion. The value of  $\Delta_f H^\circ$  for associates of bromine-containing dyes is systematically higher in comparison with associates that do not contain bromine. For example, in the case of an associate of cresolsulfonephthalein (CS) with these polymethines, the  $\lg K_{as}$  values are  $4.59 \pm 0.03$  (associate  $QB^+ \cdot CS^-$ ) and  $10.96 \pm 0.10$  (associate  $(QB^+)_2 \cdot CS^{2-}$ ), and in the case of thymolsulfonephthalein (TS) they are  $4.1 \pm 0.1$  (associate  $QR^+ \cdot TS^-$ ) and  $5.9 \pm 0.1$  (associate  $(QR^+)_2 \cdot TS^{2-}$ ) [57,60]. Obviously, bromine atoms, located in the plane of benzene rings, have virtually no effect on the geometry of BP, but significantly enhance the non-Coulomb component of intermolecular interactions, primarily the hydrophobicity of the molecule [81,82]. Thus, the introduction of halogen atoms into the structure of sulfonephthalein promotes the formation of cation-anionic associates between dyes.

## 5. Conclusions

The interaction between single- or double-charged anions of BP and cyanine cations has been investigated at dye concentrations of  $5.0 \cdot 10^{-7}$ – $4.0 \cdot 10^{-5}$  mol/L. The obtained results indicate that the processes of dye association are accompanied by a rather complex combination of different interactions, including non-Coulomb and  $\pi$ -electronic. The study of these processes is appropriate in terms of comparing the results of spectrophotometric measurements with computer simulation data.

Semi-empirical PM3 simulations are in agreement with the spectrophotometric data and indicate that the association of dye into an associate is possible and accompanied by a significant gain in energy. The study of the cation–anion association develops the concept of intermolecular interactions in solutions and creates a basis for further practical use of the spectral and equilibrium properties of associates.

Further study of the dissimilar association of dyes is aimed at finding the relationship between the structure of the dye and its ability to associate with organic ions. There is a need to develop theoretical provisions on the basis of which it would be possible to predict the stability ( $K_{as}$  values) of associates and their spectral properties based on the structure of interacting ions. Dye associates can be very useful for chemical analysis; the regulation of the completeness of the association can be considered an effective means of changing the absorption characteristics of solutions.

**Funding:** This research received no external funding.

**Institutional Review Board Statement:** Not applicable.

**Informed Consent Statement:** Not applicable.

**Conflicts of Interest:** The author declares no conflict of interest.

## References

1. Bishop, E. Observations on the theory of action of visual indicators. *Analyst* **1971**, *96*, 537–549. [[CrossRef](#)]
2. Yamamoto, K.; Adachi, K. Interaction between sulfonephthalein dyes and chitosan in aqueous solution and its application to the determination of surfactants. *Anal. Sci.* **2003**, *19*, 1133–1138. [[CrossRef](#)] [[PubMed](#)]
3. Shapovalov, S. *Association Processes with the Participation of Dyes in Solutions: Thermodynamic and Equilibrium Characteristics of Nanosystems*; Academic Publishing of European Union, OmniScriptum Publishing Group: Riga, Latvia, 2021; 124p, ISBN 978-620-2-92204-3.
4. Balderas-Hernández, P.; Ramírez-Silva, M.; Romero-Romo, M.; Palomar-Pardavé, M.; Roa-Morales, G.; Barrera-Díaz, C.; Rojas-Hernández, A. Experimental correlation between the  $pK_a$  value of sulfonphthaleins with the nature of the substituents groups. *Spectrochim. Acta A Mol. Biomol. Spectrosc.* **2008**, *69*, 1235–1245. [[CrossRef](#)]
5. Yao, W.; Byrne, R. Spectrophotometric determination of freshwater pH using bromocresol purple and phenol red. *Environ. Sci. Technol.* **2001**, *35*, 1197–1201. [[CrossRef](#)] [[PubMed](#)]
6. Yuan, S.; DeGrandpre, M.D. Evaluation of indicator-based pH measurements for freshwater over a wide range of buffer intensities. *Environ. Sci. Technol.* **2008**, *42*, 6092–6099. [[CrossRef](#)] [[PubMed](#)]
7. Martz, T.; Carr, J.; French, C.; DeGrandpre, M.D. A submersible autonomous sensor for spectrophotometric pH measurements of natural waters. *Analyt. Chem.* **2003**, *75*, 1844–1850. [[CrossRef](#)] [[PubMed](#)]
8. Maruyama, H.; Arai, F.; Fukuda, T. On-chip pH measurement using functionalized gel-microbeads positioned by optical tweezers. *Lab Chip* **2008**, *8*, 346–351. [[CrossRef](#)]
9. Kuswandi, B.; Fikriyah, C.I.; Gani, A.A. An optical fiber biosensor for chlorpyrifos using a single sol–gel film containing acetylcholinesterase and bromothymol blue. *Talanta* **2008**, *74*, 613–618. [[CrossRef](#)]
10. Zaggout, F.R. Encapsulation of bromothymol blue pH-indicator into a sol-gel matrix. *J. Dispers. Sci. Technol.* **2006**, *27*, 175–178. [[CrossRef](#)]
11. Beshir, W.B.; Eid, S.; Ebraheem, S. Use of bromocresol green dyed poly(vinyl butyral) film for dosimetric applications. *Int. J. Polym. Mater.* **2007**, *56*, 1067–1077. [[CrossRef](#)]
12. Erk, N. Spectrophotometric determination of indinavir in bulk and pharmaceutical formulations using bromocresol purple and bromothymol blue. *Pharmazie* **2004**, *59*, 183–186. [[PubMed](#)]
13. Süslü, I.; Tamer, A. Spectrophotometric determination of enoxacin as ion-pairs with bromophenol blue and bromocresol purple in bulk and pharmaceutical dosage form. *J. Pharm. Biomed. Anal.* **2002**, *29*, 545–554. [[CrossRef](#)]
14. Amin, A.; El-Fetouh Gouda, A.A.; El-Sheikh, R.; Zahran, F. Spectrophotometric determination of gatifloxacin in pure form and in pharmaceutical formulation. *Spectrochim. Acta A Mol. Biomol. Spectrosc.* **2007**, *67*, 1306–1312. [[CrossRef](#)] [[PubMed](#)]

15. Süslü, İ.; Tamer, A. Application of bromophenol blue and bromocresol purple for the extractive-spectrophotometric determination of ofloxacin. *Analyt. Lett.* **2003**, *36*, 1163–1181. [[CrossRef](#)]
16. Amin, A.S.; El-Mossalamy, M.; Killa, H.M.; Saber, A.L. Three spectrophotometric methods for the determination of oxomemazine hydrochloride in bulk and in pharmaceutical formulations using bromocresol green, congo red, and methyl orange. *Analyt. Lett.* **2008**, *41*, 80–89. [[CrossRef](#)]
17. Abdellatef, H.E. Extractive-spectrophotometric determination of disopyramide and irbesartan in their pharmaceutical formulation. *Spectrochim. Acta A Mol. Biomol. Spectr.* **2007**, *66*, 1248–1254. [[CrossRef](#)] [[PubMed](#)]
18. Rahman, N.; Ahmad Khan, N.; Hejaz Azmi, S.N. Extractive spectrophotometric methods for the determination of nifedipine in pharmaceutical formulations using bromocresol green, bromophenol blue, bromothymol blue and eriochrome black T. *Farmaco* **2004**, *59*, 47–54. [[CrossRef](#)] [[PubMed](#)]
19. Kumar, R.S.; Manjunatha, D.Y.; Shaikh, S.M.T.; Seetharamappa, J.; Harikrishna, K. Sensitive extractive spectrophotometric methods for the determination of trazodone hydrochloride in pharmaceutical formulations. *Chem. Pharm. Bull.* **2006**, *54*, 968–971. [[CrossRef](#)]
20. Onal, A.; Kepekci, S.E.; Cetin, M.; Ertuk, S. Spectrophotometric determination of certain antidepressants in pharmaceutical preparations. *J. Assoc. Off. Anal. Chem.* **2006**, *89*, 966–971.
21. Aydoğmuş, Z.; Inanlı, I. Extractive spectrophotometric methods for determination of zolmitriptan in tablets. *J. Assoc. Off. Anal. Chem.* **2007**, *90*, 1237–1241.
22. Mabrouk, M.M.; Gouda, A.A.; El-Malla, S.F.; Abdel Haleem, D.S. Sensitive spectrophotometric determination of vardenafil HCl in pure and dosage forms. *Ann. Pharm. Franç.* **2021**, *79*, 16–27. [[CrossRef](#)] [[PubMed](#)]
23. Xiong, Y.; Pei, K.; Wu, Y. Colorimetric ELISA based on glucose oxidase-regulated the color of acid–base indicator for sensitive detection of aflatoxin B1 in corn samples. *Food Control.* **2017**, *78*, 317–323. [[CrossRef](#)]
24. Nagib Qarah, A.S.; Basavaiah, K.; Swamy, N. Ion-pair extractive spectrophotometric assay of terbinafine hydrochloride in pharmaceuticals and spiked urine using bromocresol purple. *Zurn. Priklad. Spektrosk.* **2016**, *83*, 667(1)–667(9).
25. Rehman, F.; Gul, S.; Hussain, S.; Khan, S. New spectrophotometric method for the determination of mirtazapine in pharmaceutical formulations. *J. Chilean Chem. Soc.* **2016**, *61*, 2913–2915. [[CrossRef](#)]
26. Erçağ, E.; Sarioğlu, G.; Üzer, A.; Bora, T.; Apak, R. Extractive-spectrophotometric determination of amine-type stimulants and antidepressants with anionic indicator dyes. *J. Anal. Chem.* **2013**, *68*, 583–589. [[CrossRef](#)]
27. Néill, C.N.; Akdağ, M.; Betts, A.J.; Cassidy, J.F. An ammonia sensor using an unadorned bromocresol layer. *Int. J. Environ. Anal. Chem.* **2020**. [[CrossRef](#)]
28. Khattab, T.A.; Dacrorry, S.; Abou-Yousef, H.; Kamel, S. Development of microporous cellulose-based smart xerogel reversible sensor via freeze drying for naked-eye detection of ammonia gas. *Carbohydr. Polym.* **2019**, *210*, 196–203. [[CrossRef](#)]
29. Nasimov, A.M.; Isakulova, M.; Tashpulatov, K.S.; Buronov, A.O.; Mirzaev, S.E.; Toshpulatov, D.T. Photochemical studies of bromocresol purple in sol-gel membrane. *J. Adv. Res. Dynam. Control Syst.* **2020**, *12*, 1156–1159.
30. Gavrilenko, N.A.; Fedan, D.A.; Saranchina, N.V.; Sukhanov, A.V. Reversible pH-sensitive element based on bromocresol purple immobilized into the polymethacrylate matrix. *Mend. Commun.* **2018**, *28*, 450–452. [[CrossRef](#)]
31. Al-Hossainy, A.A. Combined experimental and TDDFT-DFT computation, characterization, and optical properties for synthesis of keto-bromothymol blue dye thin film as optoelectronic devices. *J. Elec. Mater.* **2021**, *50*, 3800–3813. [[CrossRef](#)]
32. Alamdari, N.E.; Aksoy, B.; Jiang, Z.; Aksoy, M.; Beck, B.H. A novel paper-based and pH-sensitive intelligent detector in meat and seafood packaging. *Talanta* **2021**, *224*, 121913. [[CrossRef](#)]
33. Ludden, M.D.; Ward, M.D. Outside the box: Quantifying interactions of anions with the exterior surface of a cationic coordination cage. *Dalton Trans. Int. J. Inorg. Chem.* **2021**, *50*, 2782–2791. [[CrossRef](#)] [[PubMed](#)]
34. Kari, N.; Koxmak, S.; Wumaier, K.; Nizamidin, P.; Abliz, S.; Yimit, A. Application of bromocresol purple nanofilm and laser light to detect mutton freshness. *Spectrochim. Acta A Mol. Biomol. Spectr.* **2021**, *244*, 118863. [[CrossRef](#)]
35. Pastrello, B.; dos Santos, G.C.; Silva-Filho, L.C.D.; de Souza, A.R.; Ximenes, V.F.; Morgon, N.H.; Ximenes, V.F. Novel amino-quinoline-based solvatochromic fluorescence probe: Interaction with albumin, lysozyme and characterization of amyloid fibrils. *Dyes Pigm.* **2020**, *173*, 107874. [[CrossRef](#)]
36. Tabaraki, R.; Sadeghinejad, N. Biosorption of six basic and acidic dyes on brown alga *Sargassum ilicifolium*: Optimization, kinetic and isotherm studies. *Water Sci. Technol.* **2017**, *75*, 2631–2638. [[CrossRef](#)] [[PubMed](#)]
37. Włodarczyk, E.; Zarzycki, P.K. Chromatographic behavior of selected dyes on silica and cellulose micro-TLC plates: Potential application as target substances for extraction, chromatographic, and/or microfluidic systems. *J. Liq. Chromatogr. Rel. Technol.* **2017**, *40*, 259–281. [[CrossRef](#)]
38. Logt, A.; Rijpma, S.; Vink, C.; Prudon-Rosmulder, E.; Wetzels, J.F.; van Berkel, M. The bias between different albumin assays may affect clinical decision-making. *Technic. Notes* **2019**, *95*, 1514–1517.
39. Zeybek, D.K.; Demir, B.; Zeybek, B.; Pekyardımcı, Ş. A sensitive electrochemical DNA biosensor for antineoplastic drug 5-fluorouracil based on glassy carbon electrode modified with poly(bromocresol purple). *Talanta* **2015**, *144*, 793–800. [[CrossRef](#)]
40. Aljerf, L. High-efficiency extraction of bromocresol purple dye and heavy metals as chromium from industrial effluent by adsorption onto a modified surface of zeolite: Kinetics and equilibrium study. *J. Environ. Manag.* **2018**, *225*, 120–132. [[CrossRef](#)]

41. Kim, Y.H.; Sathiyarayanan, G.; Kim, H.J.; Bhatia, S.K.; Seo, H.-M.; Kim, J.-H.; Song, H.-S.; Kim, Y.-G.; Park, K.; Yang, Y.-H. A liquid-based colorimetric assay of lysine decarboxylase and its application to enzymatic assay. *J. Microbiol. Biotechnol.* **2015**, *25*, 2110–2115. [[CrossRef](#)]
42. Zeng, J.; Eckenrode, H.; Dai, H.; Wilhelm, M.J. Adsorption and transport of charged vs. neutral hydrophobic molecules at the membrane of murine erythroleukemia (MEL) cells. *Coll. Surf. B Biointerf.* **2015**, *127*, 122–129. [[CrossRef](#)]
43. Thompson, S.; Ding, L.-E. Underestimation of the serum ascites albumin gradient by the bromocresol purple method of albumin measurement. *Int. Med. J.* **2018**, *48*, 1412–1413. [[CrossRef](#)]
44. Moreira, V.G.; Vaktangova, N.B.; Gago, M.D.M.; Gonzalez, B.L.; Alonso, S.G.; Rodriguez, E.F. Overestimation of albumin measured by bromocresol green vs bromocresol purple method: Influence of acute-phase globulins. *Lab. Med.* **2018**, *49*, 355–361.
45. Le Reun, E.; Leven, C.; Lapègue, M.; Kerspern, H.; Rouillé, A.; Carré, J.-L.; Padelli, M. Évaluation des performances du kit DiAgam pour le dosage immunoturbidimétrique de l'albumine plasmatique : Étude comparative. *Ann. Biol. Clin.* **2018**, *76*, 477–479.
46. Delanghe, S.; Biesen, W.; Velde, N.; Eloot, S.; Pletinck, A.; Schepers, E.; Glorieux, G.; Delanghe, J.R.; Speeckaert, M.M. Binding of bromocresol green and bromocresol purple to albumin in hemodialysis patients. *Clin. Chem. Lab. Med.* **2018**, *56*, 436–440. [[CrossRef](#)] [[PubMed](#)]
47. Pan, W.; Lau, W.; Mattman, A.; Kiaii, M.; Jung, B. Comparison of hypoalbuminemia-corrected serum calcium using BCP albumin assay to ionized calcium and impact on prescribing in hemodialysis patients. *Clin. Nephrol.* **2018**, *89*, 34–40. [[CrossRef](#)]
48. Ueno, T.; Hirayama, S.; Sugihara, M.; Miida, T. The bromocresol green assay, but not the modified bromocresol purple assay, overestimates the serum albumin concentration in nephrotic syndrome through reaction with  $\alpha_2$ -macroglobulin. *Ann. Clin. Biochem.* **2016**, *53*, 97–105. [[CrossRef](#)] [[PubMed](#)]
49. Chmelová, D.; Ondrejovič, M. Purification and characterization of extracellular laccase produced by *Ceriporiopsis subvermispora* and decolorization of triphenylmethane dyes. *J. Basic Microbiol.* **2016**, *56*, 1173–1182. [[CrossRef](#)] [[PubMed](#)]
50. Davies, D.B.; Veselkov, D.A.; Djimant, L.N.; Veselkov, A.N. Hetero-association of caffeine and aromatic drugs and their competitive binding with a DNA. *Eur. Biophys. J.* **2001**, *30*, 354–366. [[CrossRef](#)] [[PubMed](#)]
51. Davies, D.B.; Veselkov, D.A.; Veselkov, A.N. NMR determination of the hetero-association of phenanthridines with daunomycin and their competitive binding to a DNA oligomer. *Eur. Biophys. J.* **2002**, *31*, 151–162.
52. Uversky, V.N.; Winter, S.; Löber, G. Self-association of 8-anilino-1-naphthalene-sulfonate molecules: Spectroscopic characterization and application to the investigation of protein folding. *Biochim. Biophys. Acta* **1998**, *1388*, 133–142. [[CrossRef](#)]
53. Javadpour, M.M.; Barkley, M.D. Self-assembly of designed antimicrobial peptides in solution and micelles. *Biochemistry* **1997**, *36*, 9540–9549. [[CrossRef](#)]
54. Shi, X.; Ma, W.; Sun, C.; Wu, S. The aggregation behavior of collagen in aqueous solution and its property of stabilizing liposomes in vitro. *Biomaterials* **2001**, *22*, 1627–1634. [[CrossRef](#)]
55. Davies, D.B.; Veselkov, D.A.; Evstigneev, M.P.; Veselkov, A.N. Self-association of the antitumour agent novatrone (mitoxantrone) and its hetero-association with caffeine. *J. Chem. Soc. Perkin Trans.* **2001**, *2*, 61–67. [[CrossRef](#)]
56. Shapovalov, S.A.; Koval, V.L.; Chernaya, T.A.; Pereverzev, A.Y.; Derevyanko, N.A.; Ishchenko, A.A. Association of indopolymethine cyanine cations with anions of sulfonephthalein and xanthene dyes in water. *J. Braz. Chem. Soc.* **2005**, *16*, 232–240. [[CrossRef](#)]
57. Shapovalov, S.; Kiseliova, Y. Association of thymolsulfonephthalein and cresolsulfonephthalein anions with cationic cyanines in aqueous solution. *Chem. Chem. Technol.* **2010**, *4*, 271–276. [[CrossRef](#)]
58. Shapovalov, S. Association of quinaldine red cation in an aqueous solution: The interaction with anionic dyes. *AASCIT J. Nanosci.* **2017**, *3*, 35–40.
59. Shapovalov, S.; Kiseliova, Y. Heteroassociation of the bromine-containing anions of sulfophthaleins in aqueous solution. *Russ. Chem. Bull.* **2010**, *59*, 1317–1326. [[CrossRef](#)]
60. Shapovalov, S.A. Association of anions of phenolsulfonephthalein and its alkyl-substituted derivatives with single-charged cations of polymethines. *Russ. Chem. Bull.* **2011**, *60*, 465–473. [[CrossRef](#)]
61. Das Gupta, D.; Read, J.B. First pK<sub>a</sub> values of some acid-base indicators. *J. Pharm. Sci.* **1970**, *11*, 1683–1685. [[CrossRef](#)] [[PubMed](#)]
62. Herz, A. Protonation equilibria of cyanines of solution and at AgBr surfaces. *Photogr. Sci. Eng.* **1974**, *18*, 207–215.
63. Savitzky, A.; Golay, M. Smoothing and differentiation of data by simplified least squares procedures. *Analyt. Chem.* **1964**, *36*, 1627–1639. [[CrossRef](#)]
64. Paris, Q. The dual of the least-squares method. *Open J. Statist.* **2015**, *5*, 658–664. [[CrossRef](#)]
65. Shapovalov, S.A.; Samoilov, E.A. Regularities of homo- and heteroassociation of the pinacyanol cation in aqueous solution. *Russ. Chem. Bull.* **2008**, *57*, 1405–1415. [[CrossRef](#)]
66. Ishchenko, A.A.; Shapovalov, S.A. Heterogeneous association of the ions of dyes in solutions (review). *J. Appl. Spectrosc.* **2004**, *71*, 605–629. [[CrossRef](#)]
67. Shapovalov, S.A.; Svishcheva, Y.A. The peculiarities of the association between pinacyanol cations and anions in aqueous solution. *Kharkov Univ. Bull. Chem. Ser.* **2000**, *5*, 112–116. (In Russian)
68. Veselkov, D.A.; Evstigneev, M.P.; Kodintsev, V.V.; Djimant, L.N.; Davies, D.; Veselkov, A.N. Investigation of the heteroassociation of daunomycin and ethidium bromide molecules in aqueous solution by <sup>1</sup>H NMR spectroscopy. *J. Phys. Chem.* **2001**, *75*, 879–884. (In Russian)

69. Veselkov, D.A.; Sigaev, V.A.; Vysotskii, S.A.; Djimant, L.N.; Davies, D.; Veselkov, A.N. Investigation of the heteroassociation of caffeine with acridine orange dye in aqueous solution by  $^1\text{H}$  NMR spectroscopy. *J. Struct. Chem.* **2000**, *41*, 86–96. (In Russian) [[CrossRef](#)]
70. Sangster, J. Octanol-water partition coefficients of simple organic compounds. *J. Phys. Chem. Ref. Data* **1989**, *18*, 1111–1229. [[CrossRef](#)]
71. Miller, M.M.; Wasik, S.P.; Huang, G.L.; Shiu, W.Y.; Mackay, D. Relationships between octanol-water partition coefficient and aqueous solubility. *Environ. Sci. Technol.* **1985**, *19*, 522–529. [[CrossRef](#)]
72. Isac-García, J.; Dobado, J.A.; Calvo-Flores, F.G.; Martínez-García, H. Determining physical and spectroscopic properties. *Experim. Org. Chem.* **2016**, 145–175. [[CrossRef](#)]
73. Amézqueta, S.; Subirats, X.; Fuguet, E.; Rosés, M.; Ràfols, C. Octanol-water partition constant. *Liquid-Phase Extr.* **2020**, 183–208. [[CrossRef](#)]
74. Shapovalov, S.A. Interaction of cationic forms of pinacyanol with organic anions in aqueous solutions: Estimation of structural factor. *Ukr. Chem. J.* **2004**, *70*, 25–29. (In Russian)
75. Peyratout, C.; Daehne, L. Aggregation of thiocyanine derivatives on polyelectrolytes. *Phys. Chem. Chem. Phys.* **2002**, *4*, 3032–3039. [[CrossRef](#)]
76. Rubires, R.; Farrera, J.-A.; Ribo, J.M. Stirring effects on the spontaneous formation of chirality in the homoassociation of deprotonated *meso*-tetraphenylsulfonato porphyrins. *Chem. Eur. J.* **2001**, *7*, 436–446. [[CrossRef](#)]
77. Uznanski, P. From spontaneously formed aggregates to J-aggregates of photochromic spiropyran. *Synth. Metals* **2000**, *109*, 281–285. [[CrossRef](#)]
78. Tian, M.; Furuki, M.; Iwasa, I.; Sato, Y.; Pu, L.S.; Satoshi, T. Search for squaraine derivatives that can be sublimed without thermal decomposition. *J. Phys. Chem. B* **2002**, *106*, 4370–4376. [[CrossRef](#)]
79. Dewar, M.J.S.; Storch, D.M. Development and use of quantum molecular models. 75. Comparative tests of theoretical procedures for studying chemical reactions. *J. Am. Chem. Soc.* **1985**, *107*, 3898–3902. [[CrossRef](#)]
80. Stewart, J.J.P. Optimization of parameters for semiempirical methods II. Applications. *J. Comput. Chem.* **1989**, *10*, 221–264. [[CrossRef](#)]
81. Korenman, Y.I. *Extraction of Phenols*; Gor'kii, USSR; Volgo-Vyatka Publishing House: Volgo-Vyatka, Russia, 1973; 216p, ISBN 986-250-3-73314-3. (In Russian)
82. Molchanova, N.; Nielsen, J.E.; Sørensen, K.B.; Prabhala, B.K.; Hansen, P.R.; Lund, R.; Barron, A.E.; Jenssen, H. Halogenation as a tool to tune antimicrobial activity of peptoids. *Sci. Rep.* **2020**, *10*, 14805. [[CrossRef](#)] [[PubMed](#)]